The Canadian Mineralogist
Vol. 33, pp. 361-372 (1995)

CALIBRATION OF THE ION MICROPROBE FOR THE DETERMINATION OF SILVER IN PYRITE AND CHALCOPYRITE FROM THE MOBRUN VMS DEPOSIT, ROUYN–NORANDA, QUEBEC

ADRIENNE C.L. LAROCQUE*

Department of Geological Sciences, Queen's University, Kingston, Ontario K7L 3N6

JENNIFER A. JACKMAN AND LOUIS J. CABRI

CANMET, 555 Booth Street, Ottawa, Ontario K1A 0G1

C. JAY HODGSON

Department of Geological Sciences, Queen's University, Kingston, Ontario K7L 3N6

ABSTRACT

The silver contents of pyrite and chalcopyrite from the Mobrun volcanogenic massive-sulfide deposit near Noranda, Quebec, were determined using a Cameca IMS–4f ion microprobe. External standards of sulfides implanted with ^{107}Ag were used for calibration. Secondary-ion yields obtained with Cs^+ and O_2^+ primary-beam sources were compared; the highest yields and best peak/background ratio were obtained with O_2^+ and an energy offset of 90 V to eliminate mass interference by $^{75}As^{16}O_2$ and $^{75}As^{32}S$. Minimum detection-limits (MDL) of 60 ppbw were routinely obtained, and are much lower than the MDL cited by previous investigators. Silver contents range from 0.1 to 1426 ppmw in pyrite and from 1 to 200 ppmw in chalcopyrite. Au/Ag values range from 0.002 to 1.273 in pyrite and from 0.001 to 1.000 in chalcopyrite. Silver contents of primary pyrite deposited by synvolcanic hydrothermal fluids are higher than those of secondary recrystallized pyrite formed during metamorphism and deformation, indicating that metamorphic recrystallization led to the release of silver from pyrite. The remobilized silver was deposited subsequently in tectonic veins in secondary chalcopyrite and with gold as electrum.

Keywords: secondary-ion mass spectrometry, ion microprobe, relative sensitivity factor, pyrite, chalcopyrite, silver, electrum, Au/Ag values, remobilization, Mobrun, Noranda, Quebec.

SOMMAIRE

Les concentrations d'argent dans la pyrite et la chalcopyrite du gîte de sulfures massifs de Mobrun, près de Noranda, Québec, ont été déterminées avec une microsonde ionique Cameca IMS–4f. Nous avons utilisé, comme étalons externes, des sulfures implantés avec l'isotope ^{107}Ag. Nous avons dû évaluer le taux de production des ions secondaires à partir de deux sources du faisceau d'ions primaires, Cs^+ et O_2^+. C'est avec le O_2^+ que nous avons réalisé les flux et les rapports de pics à bruit de fond les plus élevés, en utilisant un décalage en énergie de 90 V pour éliminer les interférences de masse avec $^{75}As^{16}O_2$ et $^{75}As^{32}S$. Un seuil de détection minimum établi à 60 ppbw a couramment été atteint, ce qui est de beaucoup inférieur au seuil d'autres chercheurs. Les concentrations d'argent varient de 0.1 à 1426 ppmw dans la pyrite, et de 1 à 200 ppmw dans la chalcopyrite. Les valeurs Au/Ag varient de 0.002 à 1.273 dans la pyrite, et de 0.001 à 1.000 ppmw dans la chalcopyrite. Les teneurs d'argent dans la pyrite primaire, déposée par les fluides synvolcaniques hydrothermaux, sont plus élevées que celles de la pyrite recrystallisée pendant le métamorphisme et la déformation. Cette observation fait penser que l'argent a été lessivé au cours de la recristallisation métamorphique. L'argent remobilisé a par la suite été déposé dans des veines d'origine tectonique dans la chalcopyrite secondaire et sous forme d'alliage de Au–Ag (électrum).

Mots-clés: spectrométrie de masse des ions secondaires, microsonde ionique, facteur de sensibilité relative, pyrite, chalcopyrite, argent, électrum, valeur Au/Ag, remobilisation, Mobrun, Noranda, Québec.

---

* Present address: Department of Geological Sciences, The University of Manitoba, Winnipeg, Manitoba R3T 2N2.

INTRODUCTION

Silver is commonly associated with gold in many ore deposits, occurring as silver minerals or in minor amounts in sulfides, sulfosalts, native gold and gold minerals. The Au/Ag values in native gold and gold deposits exhibit specific ranges for different types of deposits. Polymetallic massive-sulfide deposits are characterized by Au/Ag values ranging from 0.006 to 1 and averaging about 0.025 (Boyle 1979). Until recently, the occurrence of gold and silver in this type of deposit was poorly understood. Early investigations of silver in sulfide minerals were based mainly on bulk chemical analysis of ore samples, concentrates and mineral separates (*e.g.*, Fleischer 1955, Hawley & Nichol 1961). Whereas these types of bulk analyses are important, they cannot provide information on the mineralogical host of silver. However, the development of trace-element microprobe techniques allows the accurate determination of precious-metal contents of minerals (Cabri 1992).

Ion-microprobe analysis of sulfide minerals has been used by process mineralogists for the characterization of sulfide ores (Chryssoulis *et al.* 1985, 1986,

TABLE 1. EXPERIMENTAL PARAMETERS FOR ION-MICROPROBE ANALYSIS

GENERAL PARAMETERS	
Instrument	Cameca IMS-4f ion microprobe
Standardization	external (ion implantation)
ION IMPLANTATION	
Ion source	low-pressure krypton dc thermal ionization source constructed at Chalk River Laboratories, Canada
Nominal ion energies	300 - 2000 keV
Operating ion energies	1 MeV
Implanted species	^{107}Ag
Implantation dose	5E14 ions/cm^2
Mineral species	pyrite, chalcopyrite
OPERATING CONDITIONS	
Beam source	O_2
Primary-ion polarity	positive
Secondary-ion polarity	positive
Primary beam current (PBC)	800 - 1200 nA
Impact energy (primary ions)	5.5 keV (10 keV PAP[1], 4.5 keV SAP[2])
Sample-charge compensation	none
Primary-beam diameter	50 - 60 μm
Crater size	approximately 200 μm x 200 μm
Analysis diameter	60 μm
Secondary detection mode	electron multiplier
Mass interferences	$^{107}AsO_2$, ^{107}AsS
Energy offset	90 V (125 V energy window)
Minimum detection limits (Ag)	60 ppb
Depth of analyzed profile	0.3 - 1.3 μm
Dynamic range (peak/background)	3 decades

[1] Primary Accelerating Potential
[2] Secondary Accelerating Potential

1987, Cabri *et al.* 1989, 1991, Chryssoulis 1990, Cabri & Chryssoulis 1990, Chryssoulis & Cabri 1990, Marion *et al.* 1991, 1992). However, the application of secondary-ion mass spectrometry (SIMS) analysis of sulfides to geological problems is more recent, and has been dominated by studies of sulfur isotopes (Eldridge *et al.* 1993, McKibben & Eldridge 1989, 1990, Layne *et al.* 1991) and gold (Arehart *et al.* 1993, Bakken *et al.* 1991, Peng 1992, Larocque *et al.* 1992, 1993b, Neumayr *et al.* 1993). Our own ion-microprobe study of gold in sulfides has provided evidence for the metamorphic remobilization of gold in the Mobrun volcanogenic massive sulfide (VMS) deposit (Larocque *et al.* 1995). The occurrence of remobilized gold with silver in electrum in tectonic veins prompted a study of the silver contents of sulfides using SIMS (Larocque *et al.* 1993c).

Ion-microprobe analysis of sulfides for their silver content has been carried out by previous investigators. For example, McIntyre *et al.* (1984) analyzed galena and sphalerite using SIMS, using energy filtering to obtain detection limits of 5 ppm for silver in sphalerite. Chryssoulis *et al.* (1986) used ion implantation to calibrate the ion microprobe for analysis of chalcopyrite, galena, sphalerite and pyrite. Detection limits of several ppm were achieved using an O^- primary beam and an energy offset of 50–100 V. Chryssoulis *et al.* (1989) produced calibration curves for silver in sphalerite, pyrite and chalcopyrite under O^- bombardment. Although ion-microprobe analysis of sulfides has been carried out previously, the procedures for analysis of pyrite and chalcopyrite for silver have not been completely documented. The purpose of this paper is to describe the analytical parameters for determination of silver in pyrite and chalcopyrite, and to present the results of analyses of these minerals from the Mobrun VMS deposit, northwestern Quebec.

Methodology

For this study, a Cameca IMS–4f ion microprobe was used to determine the silver content of pyrite and chalcopyrite in three ore lenses at the Mobrun mine (Larocque *et al.* 1995). In all, 125 analyses of pyrite in 61 sections and 43 analyses of chalcopyrite in 29 sections were carried out. Experimental parameters are summarized in Table 1. External standards of pyrite and chalcopyrite were implanted with ^{107}Ag for calibration. Implantation doses of ^{107}Ag were not verified; however, verification of implantation doses of ^{197}Au yielded results within 5% of the expected dose (Larocque 1993). As the implantation dose is used to calibrate analysis of unknowns, the accuracy of analysis is assumed to be ±5%. In natural samples, two isotopes of silver are present in nearly equal proportions (51.83 wt.% ^{107}Ag and 48.17 wt.% ^{109}Ag). Therefore, below the implanted layer, the background concentrations of the two species should be about equal [*i.e.*, the depth profiles should merge (Fig. 1)].

Prior to analysis, it was necessary to establish optimum operating conditions. Interfering species $^{107}(AsO_2)$ ($^{75}As^{16}O_2$) and $^{107}(AsS)$ ($^{75}As^{32}S$) have masses too close to that of ^{107}Ag to resolve by operating in high-mass-resolution mode, as was done for gold analysis (Larocque *et al.* 1995). Therefore, the alternative method of energy filtering (Shimizu *et al.* 1978) was employed to remove isobaric interferences at masses 107 and 109. Depth profiles were acquired

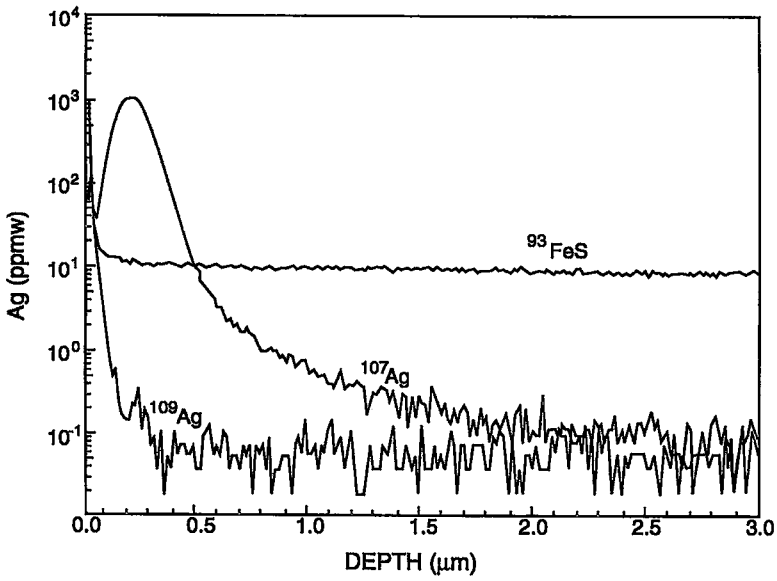

FIG. 1. Depth profile through pyrite standard implanted with ^{107}Ag, using an O_2^+ primary beam and an energy offset of 90 V.

TABLE 2. SECONDARY COUNTS OF ^{107}Ag WITH Cs^+ AND O_2^+ BOMBARDMENT

Incident Beam	Cs^+ (100 nA PBC[1])			O_2^+ (1000 nA PBC)		
Energy Offset	Peak[2]	Background[3]	Pk/Bg	Peak[2]	Background[3]	Pk/Bg
50V	2.0E5	7.0E4	2.9E0	1.1E5	2.0E2	5.5E2
75V	1.5E3	1.0E1	1.5E2	3.0E4	2.0E1	1.5E3
90V	1.2E3	2.2E0	5.5E2	1.5E5	3.0E0	3.3E4
100V	1.0E3	2.0E0	5.0E2	1.1E4	1.0E0	1.1E4

[1] Primary beam current
[2] measured from the peak of the ^{107}Ag profile in implanted pyrite
[3] measured from the ^{107}Ag depth profile, below the implanted layer

using several energy-offsets (50, 75, 90 and 100 V), using both Cs^+ and O_2^+ as primary beam sources operating at 10 keV acceleration potential. The results are summarized in Table 2. Cs^+ bombardment is known to result in high yields of secondary ions for gold, and bombardment by Cs^+ and O^- should produce comparable yields of secondary silver ions (Storms *et al.* 1977). However, our results indicate that the highest intensity and greatest dynamic range (peak/background) for ^{107}Ag were obtained with O_2^+ bombardment and an energy offset of 90 V (Fig. 1).

Operating under these conditions with an average primary-beam current of 1000 nA, we were able to achieve minimum detection-limits (MDL) for silver of 60 ppbw, which is much lower than the MDL cited by previous workers. Secondary counts of ^{109}Ag and $^{93}(FeS)$ ($^{57}Fe^{36}S$) were monitored to ensure instrumental stability and sample homogeneity. Software produced by Charles Evans and Associates (version 3.0) was used to reduce the raw peak-count data to concentrations of silver in parts per million by weight (*i.e.*, μg/g). The details of data reduction are summarized in Appendix 1.

Sample Description

Samples of mineralization were collected from the Mobrun mine in the Abitibi greenstone belt. The geological setting of the Mobrun deposit has been described by Caumartin & Caillé (1990), Riopel *et al.* (1990) and Barrett *et al.* (1992), among others. The deposit is hosted by Archean felsic-to-mafic volcanic rocks that have undergone greenschist-facies metamorphism and two main periods of deformation (Dimroth *et al.* 1983a, b). It consists of three main orebodies (the Main, Satellite and 1100 lenses), with Au/Ag values ranging from 0.04 to 0.12 and averaging 0.05 (see Larocque *et al.* 1995, Table 1). These values are higher than the average for polymetallic deposits (Boyle 1979), and in the upper 30% for VMS deposits in the eastern Abitibi Subprovince that contain silver and gold (Chartrand & Cattalani 1990).

The Mobrun orebodies contain major pyrite, sphalerite, chalcopyrite and pyrrhotite, minor galena and magnetite, and trace arsenopyrite, digenite, tetrahedrite and electrum (Fig. 2). Larocque *et al.* (1993a, 1995) identified a number of facies of mineralization based on mineralogical, textural, and structural characteristics. The facies have been subdivided into primary facies, which resulted from synvolcanic deposition and "zone refining" of sulfides by hydrothermal fluids (Eldridge *et al.* 1983), and secondary facies, which formed as a result of metamorphism and deformation. Because of their volumetric importance in the orebodies, we analyzed mainly granular pyrite (Fig. 2A) and massive pyrite (Figs. 2B, C) by SIMS. In addition, ion-microprobe analysis has been carried out on coarse euhedral pyrite (Fig. 2D) and chalcopyrite (Fig. 2E) in secondary veins.

At Mobrun, metamorphic recrystallization led to the release of invisible gold from primary pyrite and subsequent deposition of remobilized gold in electrum and chalcopyrite in secondary veins (Larocque *et al.* 1995). The compositions of electrum (determined by electron-microprobe analysis) occupy three distinct but overlapping ranges (Larocque 1993). The average Au/Ag values of electrum are 0.65 for the 1100 lens, 1.04 for the Main lens, and 2.03 for the Satellite lens complex. These values are much lower than those for native gold and Au–Ag alloys in Kuroko-type polymetallic deposits and in gold-only deposits in the Abitibi (Boyle 1979).

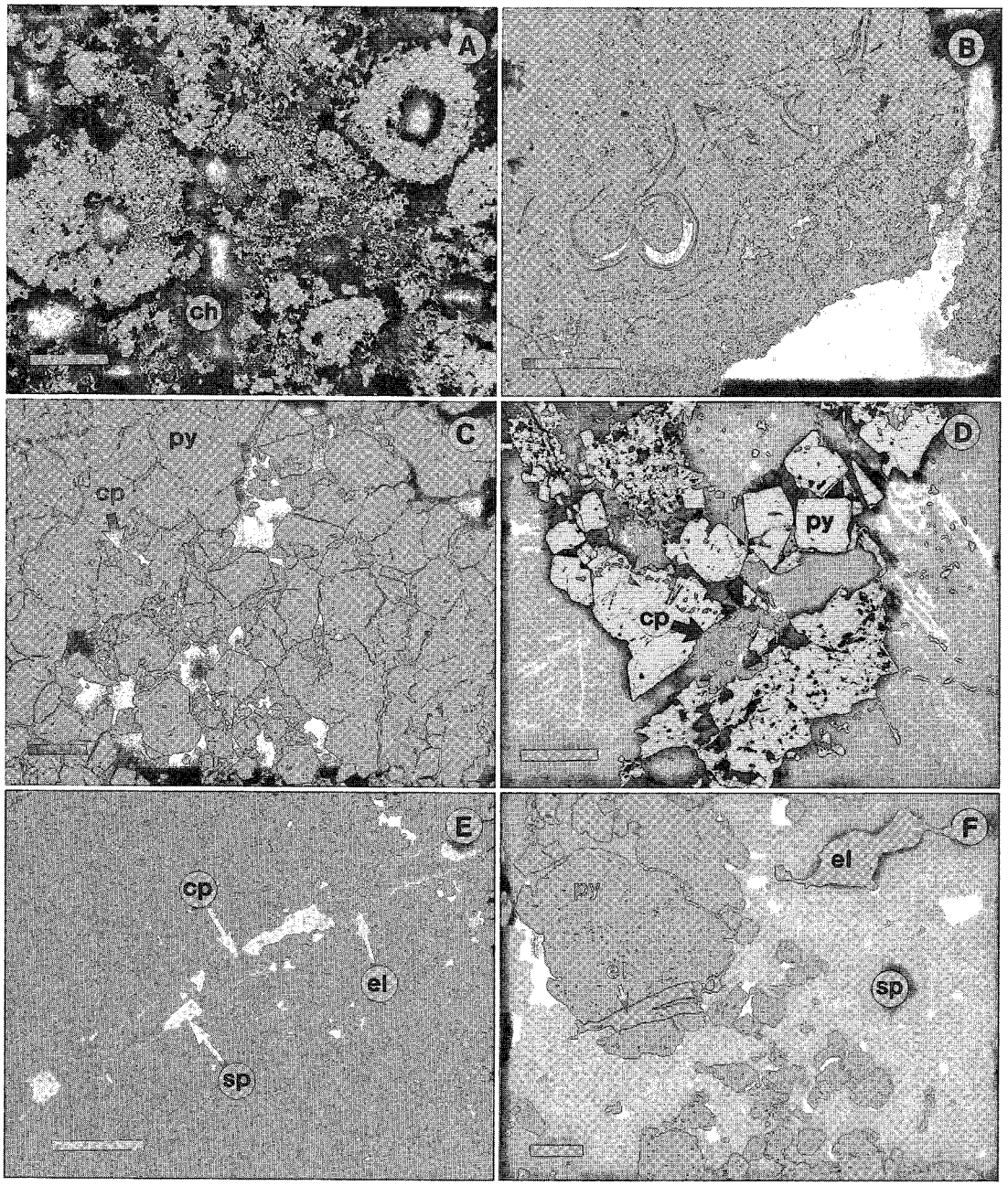

FIG. 2. Reflected-light photomicrographs of facies of mineralization from the Mobrun deposit. Abbreviations are as follows: pyrite (py), chalcopyrite (cp), sphalerite (sp), electrum (el), chlorite (ch). Length of scale bar is shown in parentheses. (A) Granular pyrite with concentric internal structure in matrix of chlorite (500 μm). (B) Massive fine pyrite with colloform banding (500 μm). (C) Massive coarse (recrystallized) pyrite with chalcopyrite replacing grain boundaries (100 μm). (D) Coarse euhedral pyrite with chalcopyrite in carbonate vein (500 μm). (E) Massive fine pyrite cut by secondary vein containing chalcopyrite, sphalerite, and electrum (100 μm). (F) Vein of electrum cutting granular pyrite in sphalerite matrix (250 μm).

RESULTS

Pyrite

The silver content of pyrite ranges from 0.6 to 500 ppmw (average 33.6 ppmw) in the Main lens, from 0.1 to 1426 ppmw (average 39.7 ppmw) in the Satellite lens complex, and from 1.1 to 570 ppmw (average 56.3 ppmw) in the 1100 lens. The average content of silver for all samples from all orebodies is 42.1 ppmw. The frequency-distribution diagrams of silver content of pyrite in the Main and Satellite lenses show a log-normal distribution, with maxima in the 8 – 16 ppmw range (Fig. 3). The histogram for silver content of pyrite in the 1100 lens shows a bimodal distribution, with a principal maximum in the 8 – 16 ppmw range and a subordinate maximum in the 128 – 256 ppmw range (Fig. 3).

As in the case of gold, depth profiling has revealed that silver occurs in two forms, as very fine colloid-size or structurally bound silver within pyrite, and in sub-microscopic inclusions of electrum (the silver contents in Figs. 3, 4 and 7 and Table 3 represent the former).

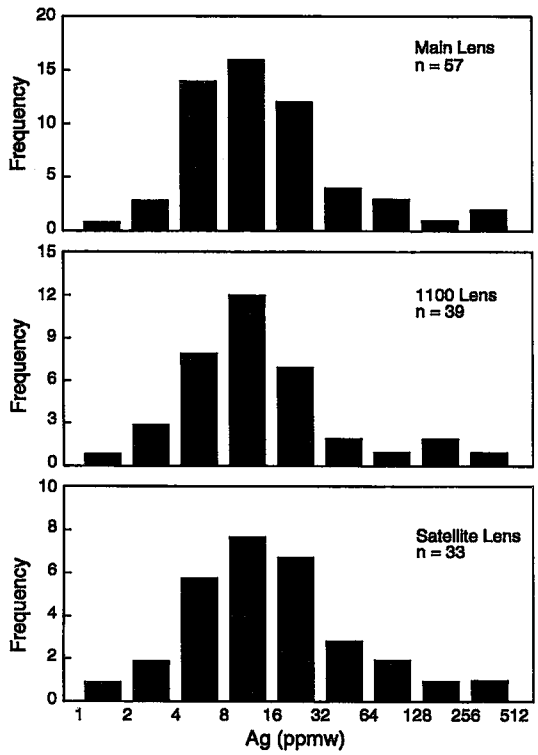

FIG. 3. Frequency distribution of silver content of pyrite from the Mobrun orebodies, as determined by SIMS.

There is a large range in silver content of pyrite among samples, owing to the bulk zonation of silver throughout each orebody. The range of silver content in pyrite in individual hand-specimens and thin sections is summarized in Table 3. Compositions of inclusion-free massive fine pyrite show the greatest consistency in concentrations of silver.

Larocque *et al.* (1995) demonstrated that secondary recrystallized pyrite has lower concentrations of gold than associated primary pyrite. Similarly, recrystallized pyrite contains less silver than associated primary pyrite (Fig. 4). Concentrations of silver in recrystallized granular and nodular pyrite are between 13 and 67% of those in unrecrystallized granular and nodular pyrite. Recrystallized massive pyrite has concentrations of silver between 1 and 71% of those in primary massive pyrite. Coarse euhedral pyrite in secondary veins contains between 1 and 36% of the silver in the associated primary pyrite.

Au/Ag values in pyrite (Fig. 5) range from 0.003 to 0.500 (average 0.101) in the Main lens, from 0.002 to 0.600 (average 0.048) in the Satellite lens complex, and from 0.003 to 1.273 (average 0.067) in the 1100 lens. The average ratio for all samples from all of the orebodies (0.073) is similar to that for the deposit as a whole (0.050). In most samples, Au/Ag is lower in recrystallized pyrite than in associated primary pyrite, and the lowest Au/Ag values pertain mainly to recrystallized pyrite (Fig. 6). The ratio between gold and silver released during recrystallization of pyrite ranges from 0.013 to 0.900 and averages 0.204 (Larocque 1993, Table 5.4).

Chalcopyrite

Chalcopyrite in primary stringer mineralization and inclusions in primary pyrite, and coarse-grained chalcopyrite in secondary veins were analyzed. The silver content of chalcopyrite ranges from 1 to 200 ppmw (average 29 ppmw), with a maximum in the range 16 to 32 ppmw (Fig. 7). Au/Ag values range from 0.001 to 1.000 (average 0.073) with a maximum in the range 0.016 – 0.032 (Fig. 8). The highest concentrations of silver (Larocque 1993) and lowest Au/Ag values are associated with secondary chalcopyrite (Fig. 8).

DISCUSSION

Silver is present in consistently lower concentrations in secondary pyrite than in associated primary pyrite, as is the case for gold (Larocque *et al.* 1995). This indicates that metamorphic recrystallization resulted in the release of silver from pyrite. Some of the remobilized silver was deposited along with gold as secondary electrum in tectonic veins. However, the Au/Ag values of electrum are high (*i.e.*, the electrum is gold-rich, silver-poor) relative to the ratio of gold to silver released during metamorphic recrystallization of pyrite

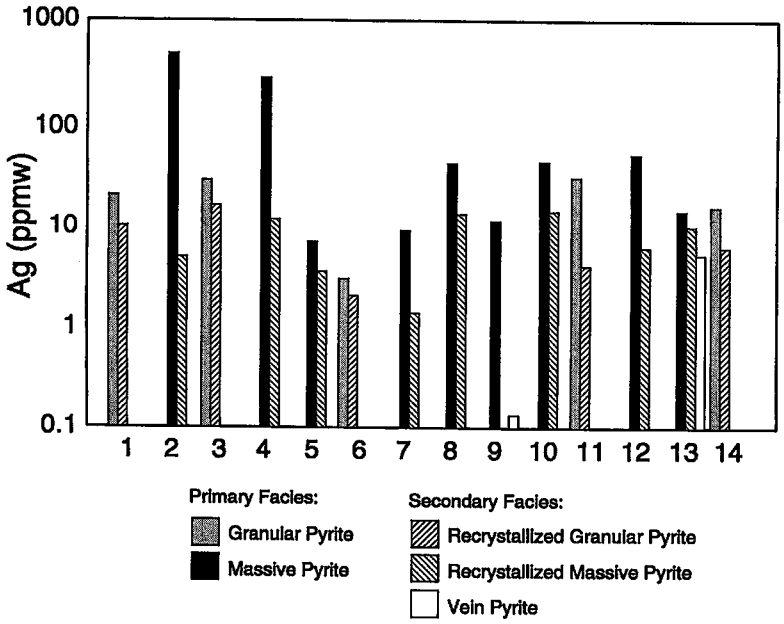

FIG. 4. Silver content of pyrite in various facies of mineralization coexisting within individual thin sections, as determined by SIMS.

TABLE 3. RANGE OF SILVER-CONTENT OF PYRITE (BY SIMS)

	Pyrite-Bearing Facies	Number of Analyses	Average Silver-Content (ppmw)	Mean Deviation (ppmw)	% Deviation
Main Lens					
1	granular	2	6.5	0.5	8
2	massive with inclusions	2	8.0	0.0	0
3	massive fine py	2	23.0	4.0	17
4	massive fine py with inclusions	2	321.5	178.5	56
5	massive fine py with inclusions	2	196.0	89.0	45
6	massive fine py	2	7.0	0.0	0
7	massive fine py with inclusions	2	10.5	4.5	43
8	nodular py	2	12.5	1.5	12
9	granular py	2	4.1	0.1	2
10*	massive fine py	2	9.0	3.0	33
11	massive fine py	3	29.0	0.0	0
Satellite Lens Complex					
1	granular py with inclusions	3	22.7	3.2	14
2	granular py with inclusions	2	9.0	5.0	56
3	granular py	2	2.6	0.4	15
4	massive fine py with inclusions	2	9.0	2.0	22
5	granular py	2	21.0	0.0	0
6	granular py with inclusions	2	8.3	0.3	3
7	massive fine py with inclusions	2	10.0	1.0	10
1100 Lens					
1	massive recrystallized py with cpy	2	552.5	17.5	3
2	massive recrystallized py	2	14.5	0.5	3
3	massive fine py with inclusions	2	13.0	3.0	23
4	foliated py	2	19.5	8.5	44
5	massive recrystallized py	2	7.5	2.5	33
6	massive fine py	2	15.0	0	0

* same hand specimen as thin section listed immediately below

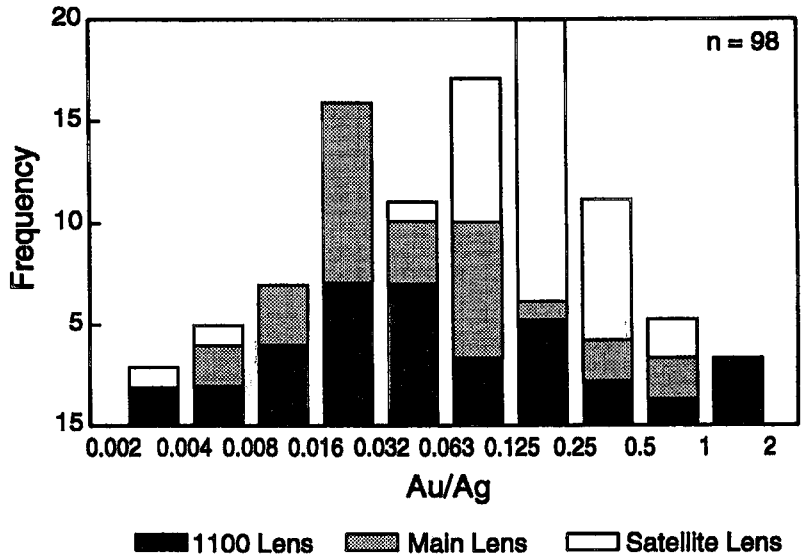

FIG. 5. Frequency distribution of Au/Ag in pyrite from the Mobrun deposit, as determined by SIMS.

(Larocque 1993). The analysis of chalcopyrite suggests that remobilized silver was incorporated preferentially into secondary chalcopyrite in veins, resulting in lower silver content and higher Au/Ag values than expected in the associated electrum. The evidence for remobilization of gold and silver within the Mobrun orebodies has important implications for the formation of late vein-gold deposits that are spatially associated with VMS deposits in the eastern Abitibi belt.

CONCLUSIONS

(1) Mass interference by $^{75}As^{16}O_2$ and $^{75}As^{32}S$ were eliminated using conventional energy-filtering.
(2) The highest secondary-ion intensity and greatest peak/background ratio in external implanted standards were achieved with O_2^+ bombardment and a 90 V sample offset. Minimum limits of detection of 60 ppbw were routinely obtained.

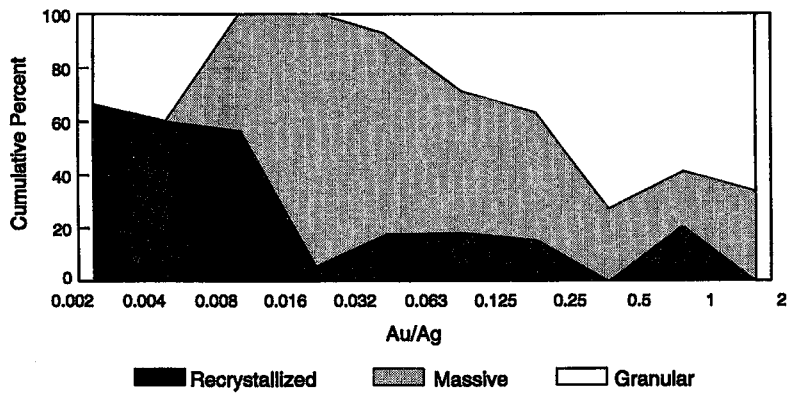

FIG. 6. Diagram showing, in cumulative percent, the proportions of various pyrite-bearing facies in each Au/Ag range in Figure 5. "Recrystallized" includes recrystallized (secondary) massive and granular pyritic mineralization and euhedral pyrite in secondary veins. "Massive" and "granular" refer to primary pyrite-bearing facies.

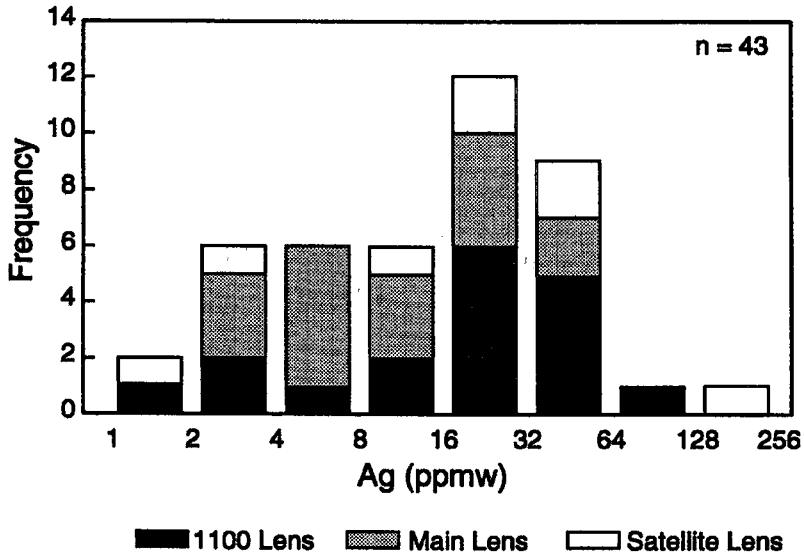

FIG. 7. Frequency distribution of silver content of chalcopyrite from the Mobrun deposit, as determined by SIMS.

(3) Silver is present in pyrite in submicroscopic inclusions of electrum and as fine colloid-size or structurally bound silver.
(4) Metamorphic recrystallization resulted in the release of silver from primary pyrite, and its subsequent deposition in secondary electrum and chalcopyrite in tectonic veins. Preferential incorporation of remobilized silver into secondary chalcopyrite accounts for the higher Au/Ag values than expected in the associated electrum.
(5) The Au/Ag values in pyrite range from 0.002 to 1.273, with an average value of 0.073, similar to that of the deposit as a whole.
(6) The determination of gold and silver contents of sulfide minerals and subsequent calculation of Au/Ag values for sulfides fills a gap between documented values in native gold and in gold deposits.

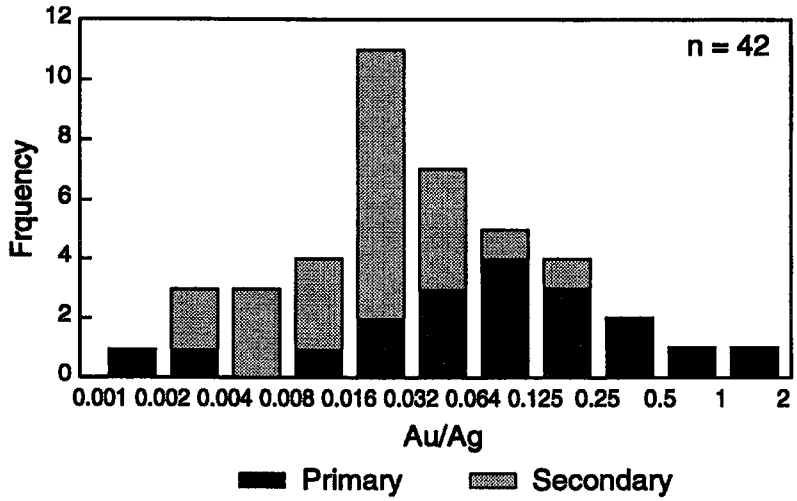

FIG. 8. Frequency distribution of Au/Ag in chalcopyrite from the Mobrun deposit, as determined by SIMS.

ACKNOWLEDGEMENTS

We thank employees of Ressources Audrey Inc. and Mine Mobrun, especially Michel Bouchard and Pierre-Jean Lafleur. Vic Chartrand of CANMET provided capable technical assistance with ion-microprobe analyses. The manuscript was prepared while the first author was a guest scientist in Earth and Environmental Sciences (EES) Division at Los Alamos National Laboratory (LANL), New Mexico. Logistical support provided by EES–1 is greatly appreciated. In particular, ACLL is grateful to Fraser Goff for his sponsorship and to Jim Stimac for providing access to a photographic microscope. Eric Montoya (EES–1) and Ruth Bigio (EES–4) carried out computer-aided drafting of figures. We are indebted to two anonymous reviewers, Associate Editor Frank Hawthorne and Editor Robert Martin for comments that improved the manuscript. Financial support was provided by Ressources Audrey Inc., Minnova Inc., and NSERC, through a Collaborative Research and Development Grant awarded to CJH.

REFERENCES

AREHART, G.B., CHRYSSOULIS, S.L. & KESLER, S.E. (1993): Gold and arsenic in iron sulfides from sediment-hosted disseminated gold deposits: implications for depositional processes. *Econ. Geol.* **88**, 171-185.

BAKKEN, B.M., BRIGHAM, R.H. & FLEMING, R.H. (1991): The distribution of gold in unoxidized ore from Carlin-type deposits revealed by secondary ion mass spectrometry (SIMS). *Geol. Soc. Am., Program Abstr.* **23**, A228.

BARRETT, T.J., CATTALANI, S., HOY, L., RIOPEL, J. & LAFLEUR, P.J. (1992): Massive sulfide deposits of the Noranda area, Quebec. IV. The Mobrun mine. *Can. J. Earth Sci.* **29**, 1349-1374.

BOYLE, R.W. (1979): The geochemistry of gold and its deposits. *Geol. Surv. Can., Bull.* **280**.

CABRI, L.J. (1992): The distribution of trace precious metals in minerals and mineral products. *Mineral. Mag.* **56**, 289-308.

_____ & CHRYSSOULIS, S.L. (1990): Advanced methods of trace-element microbeam analyses. *In* Advanced Microscopic Study of Ore Minerals (J.L. Jambor & D.J. Vaughan, eds.). *Mineral. Assoc. Can., Short-Course Handbook* **17**, 341-377.

_____, _____, CAMPBELL, J.L. & TEESDALE, W.J. (1991): Comparison of *in-situ* gold analyses in arsenian pyrite. *Appl. Geochem.* **6**, 225-230.

_____, _____, DE VILLIERS, J.P.R., LAFLAMME, J.H.G. & BUSECK, P.R. (1989): The nature of "invisible" gold in arsenopyrite. *Can. Mineral.* **27**, 353-362.

CAUMARTIN, C. & CAILLÉ, M.-F. (1990): Volcanic stratigraphy and structure of the Mobrun mine. *In* The Northwestern Quebec Polymetallic Belt: A Summary of 60 Years of Mining Exploration (M. Rive, P. Verpaelst, Y. Gagnon, J.-M. Lulin, G. Riverin & A. Simard, eds.). *Can. Inst. Min. Metall., Spec. Vol.* **43**, 119-132.

CHARTRAND, F. & CATTALANI, S. (1990): Massive sulfide deposits in northwestern Quebec. *In* The Northwestern Quebec Polymetallic Belt: A Summary of 60 Years of Mining Exploration (M. Rive, P. Verpaelst, Y. Gagnon, J.-M. Lulin, G. Riverin & A. Simard, eds.). *Can. Inst. Min. Metall., Spec. Vol.* **43**, 77-91.

CHRYSSOULIS, S.L. (1990): Quantitative trace precious metal analysis of sulfide and sulfarsenide minerals by SIMS. *In* Secondary Ion Mass Spectrometry, SIMS VII Int. Conf. Proc. (A. Benninghoven, C.A. Evans, K.D. McKeegan, H.A. Storms & H.W. Werner, eds.). John Wiley & Sons, Ltd., Chichester, U.K. (405-408).

_____ & CABRI, L.J. (1990): Significance of gold mineralogical balances in mineral processing. *Inst. Min. Metall., Trans.* **99**, C1-10.

_____, _____ & LENNARD, W. (1989): Calibration of the ion microprobe for quantitative trace precious metal analyses of ore minerals. *Econ. Geol.* **84**, 1684-1689.

_____, _____ & SALTER, R.S. (1987): Direct determination of invisible gold in refractory sulfide ores . *In* Proc. Int. Symp. on Gold Metallurgy 1 (R.S. Salter, D.M. Wyslouzil & G.W. McDonald, eds.). *Proc. Metall. Soc., Can. Inst. Min. Metall.* (235-244).

_____, CHAUVIN, W.J. & SURGES, L.J. (1986): Trace element analysis by secondary ion mass spectrometry with particular reference to silver in the Brunswick sphalerite. *Can. Metall. Quart.* **25**, 233-239.

_____, SURGES, L.J. & SALTER, R.S. (1985): Silver mineralogy at Brunswick Mining and Smelting Corporation, Ltd. *In* Complex Sulfides (A.D. Zunkel, R.S. Boorman, A.E. Morris & R.J. Wesley, eds.). The Metall. Soc., Am. Inst. Mining Engineers, Warrendale, Pennsylvania (815-830).

DIMROTH, E., IMREH, L., GOULET, N. & ROCHELEAU, M. (1983a): Evolution of the south-central segment of the Archean Abitibi Belt, Québec. II. Tectonic evolution and geomechanical model. *Can. J. Earth Sci.* **20**, 1355-1373.

_____, _____, _____ & _____ (1983b): Evolution of the south-central segment of the Archean Abitibi Belt, Québec. III. Plutonic and metamorphic evolution and geotectonic model. *Can. J. Earth Sci.* **20**, 1374-1388.

ELDRIDGE, C.S., BARTON, P.B., JR. & OHMOTO, H. (1983): Mineral textures and their bearing on formation of the Kuroko orebodies. *Econ. Geol., Monogr.* **5**, 241-281.

_____, WILLIAMS, N. & WALSHE, J.L. (1993): Sulfur isotope variability in sediment-hosted massive sulfide deposits as determined using the ion microprobe SHRIMP.

II. A study of the H.Y.C. deposit at McArthur River, Northern Territory, Australia. *Econ. Geol.* **88**, 1-26.

FLEISCHER, M. (1955): Minor elements in some sulfide minerals. *Econ. Geol., 50th Anniv. Vol.*, 970-1024.

HAWLEY, J.E. & NICHOL, I. (1961): Trace elements in pyrite, pyrrhotite, and chalcopyrite of different ores. *Econ. Geol.* **56**, 467-487.

LAROCQUE, A.C.L. (1993): *The Geological Controls of Gold Distribution in the Mobrun Volcanic-Associated Massive Sulfide Deposit, Rouyn–Noranda, Quebec.* Ph.D. thesis, Queen's University, Kingston, Ontario.

_____, CABRI, L.J., JACKMAN, J.A. & HODGSON, C.J. (1993c): SIMS analysis of Ag in pyrite: experimental parameters and preliminary results. *Geol. Assoc. Can. – Mineral. Assoc. Can., Program Abstr.* **18**, A56.

_____, HODGSON, C.J., CABRI, L.J. & JACKMAN, J.A. (1992): Application of SIMS analysis of pyrite to the study of metamorphic remobilization of Au in the Mobrun VMS deposit, Rouyn–Noranda, Quebec. *Geol. Assoc. Can. – Mineral. Assoc. Can., Program Abstr.* **17**, A63.

_____, _____, _____ & _____ (1993b): Ion-microprobe study of sulfide minerals from the Mobrun VMS deposit in northwestern Quebec: evidence for metamorphic remobilization of Au. *Geol. Assoc. Can. – Mineral. Assoc. Can., Program Abstr.* **18**, A56.

_____, _____, _____ & _____ (1995): Ion-microprobe analysis of pyrite, chalcopyrite and pyrrhotite from the Mobrun VMS deposit in northwestern Quebec: evidence for metamorphic remobilization of Au. *Can. Mineral.* **33**, 373-388.

_____, _____ & LAFLEUR, P.-J. (1993a): Gold distribution in the Mobrun volcanic-associated massive sulfide deposit, Noranda, Quebec: a preliminary evaluation of the role of metamorphic remobilization. *Econ. Geol.* **88**, 1443-1459.

LAYNE, G., HART, S.R. & SHIMIZU, N. (1991): Microscale lead and sulfur isotope zonation in hydrothermal sulfides by ion microprobe: new findings from the Mississippi Valley-type Pb–Zn deposits of the Viburnum Trend, S.E. Missouri. *Geol. Soc. Am., Program Abstr.* **23**, A101-A102.

MARION, P., HOLLIGER, P., BOIRON, M.C., CATHELINEAU, M. & WAGNER, F.E. (1991): New improvements in the characterization of refractory gold in pyrites: an electron microprobe, Mössbauer spectrometry and ion microprobe study. *Proc. Brazil Gold '91* (E.A. Ladeira, ed.), Balkema, Rotterdam, The Netherlands (389-395).

_____, MONROY, M., HOLLIGER, P., BOIRON, M.C., CATHELINEAU, M., WAGNER, F.E. & FRIEDL, J. (1992): Gold-bearing pyrites: a combined ion microprobe and Mössbauer spectrometry approach. *In* Source, Transport, and Deposition of Metals (M. Pagel & J.L. Leroy, eds.). Balkema, Rotterdam, The Netherlands.

MCINTYRE, N.S., CABRI, L.J., CHAUVIN, W.J. & LAFLAMME, J.H.G. (1984): Secondary ion mass spectrometric study of dissolved silver and indium in sulfide minerals. *Scanning Elect. Micros.* **3**, 1139-1146.

MCKIBBEN, M.A. & ELDRIDGE, C.S. (1989): Sulfur isotopic variations among minerals and aqueous species in the Salton Sea geothermal system: a SHRIMP ion-microprobe and conventional study of active ore genesis in a sediment-hosted environment. *Am. J. Sci.* **289**, 661-707.

_____ & _____ (1990): Radical sulfur isotope zonation of pyrite accompanying boiling and epithermal gold deposition: a SHRIMP study of the Valles Caldera, New Mexico. *Econ. Geol.* **85**, 1917-1925.

NEUMAYR, P., CABRI, L.J., GROVES, D.I., MIKUCKI, E.J. & JACKMAN, J.A. (1993): The mineralogical distribution of gold and relative timing of gold mineralization in two Archean settings of high metamorphic grade in Australia. *Can. Mineral.* **31**, 711-725.

PENG, SHA (1992): SIMS analyses of gold in iron sulfides from the Gold Quarry Deposit, Nevada. *Geol. Soc. Am., Program Abstr.* **24**, A315-A316.

RIOPEL, J., HUBERT, C., CATTALANI, S., BARRETT, T.J. & MACLEAN, W.H. (1990): *Métallogénie des Gisements de Métaux Usuels dans la Ceinture de Roches Vertes de l'Abitibi, Nord-Ouest Québécois. IV. La Mine Mobrun, Lentille Principale, Noranda, Québec.* IREM Projet No. 82-43G, 1988-89, Ministère de l'Energie et des Ressources, Québec.

SHIMIZU, N., SEMET, M.P. & ALLÈGRE, C.J. (1978): Geochemical applications of quantitative ion-microprobe analysis. *Geochim. Cosmochim. Acta* **42**, 1321-1334.

STORMS, H.A., BROWN, K.F. & STEIN, J.D. (1977): Evaluation of a cesium positive ion source for secondary ion mass spectrometry. *Anal. Chem.* **49**, 2023-2030.

Received June 10, 1993, revised manuscript accepted February 18, 1994.

APPENDIX 1.
CALCULATION OF RELATIVE SENSITIVITY AND CONVERSION FACTORS

During ion-microprobe analysis, secondary-ion counts of a given mass were measured. Charles Evans and Associates software (version 3.0) was used to reduce the data. By integrating under the depth-profile curve for implanted standards (*e.g.*, Fig. 1) and inputting the known implantation dose, a relative sensitivity factor (RSF) was obtained. The RSF is specific to the matrix species monitored, and is determined by the following relationship:

$$RSF = Conc_{Au}/Counts_{Au} \times Counts_{Matrix}$$

where the concentration of Au is in ions/cm^3, and counts refer to secondary-ion counts of Au and the matrix species, all in the implanted standard. Using the RSF, it was possible to calculate the concentration of silver in atoms/cm^3. In order to obtain results in ppmw (*i.e.*, μg/g), it is necessary to calculate a conversion factor. A sample calculation for silver in pyrite is summarized below.

Molecular weight of pyrite = 119.98 g/mol
Atomic weight of ^{107}Ag = 106.91 g/mol
Density of pyrite = 5.0 g/cm^3
Avogadro's number = 6.02×10^{23} molecules/mol
Molecular density of pyrite:
(5.0 g/cm^3 $\times$ 6.02×10^{23} molecules/mol)/119.98 g/mol = 2.51×10^{22} molecules/cm^3.
Atomic density of pyrite:
2.51×10^{22} molecules/cm^3 $\times$ 3 atoms/molecule = 7.53×10^{22} atoms/cm^3
Thus, 1 part per million atomic (ppma) in pyrite = 7.53×10^{16} atoms/cm^3
Average atomic weight of pyrite:
119.98 g/mol / 3 = 39.99 g/mol
Concentration (by weight) of ^{107}Ag in pyrite:
1 ppma = 106.91 g/mol / 39.99 g/mol = 2.67 ppmw (or μg/g)

Since 1 ppma = 7.53×10^{16} atoms/cm^3, then 1 part per million weight (ppmw) = 7.53×10^{16} / 2.67 = 2.82×10^{16} atoms/cm^3.

Thus, to calculate the conversion factor to be used by the software to determine the concentration of ^{107}Ag in pyrite, the RSF was divided by 2.82×10^{16} atoms/cm^3. As two isotopes of silver are present in nearly equal proportions in natural samples, measured concentrations of ^{107}Ag were multiplied by 2 to give the total concentration of silver in each of the Mobrun samples. For this study, ^{93}(FeS) (^{57}Fe^{36}S) was monitored as a matrix mass. The RSFs for ^{107}Ag were found to range from 5.27×10^{18} to 2.34×10^{19} atoms/cm^3 or 187 to 830 ppmw with respect to ^{93}(FeS).